EXPLORING THE COMBUSTION CHARACTERISTICS OF TURBULENT PREMIXED AMMONIA/HYDROGEN/AIR FLAMES VIA DTF MODEL-BASED LARGE EDDY SIMULATION

Ping WANG [1,2,*], Zeyu ZHANG[1], Zhengchun YANG [1], Subhajit ROY [1], Weijia QIAN [1],

Kang CHENG[1]

[*1] Institute for Energy Research, Jiangsu University, Zhenjiang, Jiangsu, 212013, China

[2] State Key Laboratory of Clean Energy Utilization, Zhejiang University, Hangzhou Zhejiang, 310058, China

[*] Corresponding author; E-mail: pingwang@ujs.edu.cn

This study aims to investigate the combustion characteristics of a premixed swirl flame for a fuel mixture made of ammonia and hydrogen. The use of NH_3 and H_2 as carbon-free fuels in combustion systems can significantly reduce greenhouse gas emissions. Blending ammonia with hydrogen is a promising approach to enhance hydrogen combustion safety and ammonia combustion intensity. A three-dimensional large eddy simulation using a DTF model was run in order to get extensive and multi-scale information regarding the flow and reacting field of a premixed swirl flame using a 50% NH_3/50% H_2 fuel blend. The findings indicate that whereas NO is created near the flame front, OH radicals are mostly synthesized in the inner recirculation zone. The fuel-NO pathway, which is sensitive to flame temperature, is what causes NO to be produced. The flame position is where the recirculation zone lies, and the total recirculation strength is determined by the inner recirculation strength. The prediction of NO concentration by LES, considering heat loss, is closer to the experimental value. The chemically reacting network simulation can precisely estimate NO emission by considering the heat loss ratio and the recirculation strength calculated by LES. Overall, this study provides valuable insights into the combustion characteristics of an ammonia/hydrogen fuel blend, which could contribute to the development of cleaner and more efficient combustion technologies. The findings of this study can be of great significance in the fields of sustainable energy and environmental protection.

Key words*: Low carbon fuel, DTF model, Ammonia combustion, LES, Turbulent flame*

1. Introduction

It is now widely acknowledged that global warming, which is caused by CO_2 emissions, is an urgent problem. A sizable percentage of these emissions have been caused by fossil fuels, which constitute the main source of energy for industrial and human activity globally. As a result, the use of

carbon-free fuels is necessary to reduce CO_2 emissions. To achieve this, significant research efforts are required in developing and implementing such fuels.

The unique feature of ammonia (NH_3), which causes it to solely produce water and nitrogen as combustion byproducts when entirely burned, has recently drawn the attention of researchers. Furthermore, ammonia is a viable hydrogen energy vector because its molecules can store an enormous amount of hydrogen, up to 17.7% [1]. Ammonia has been used as a chemical fertilizer for more than a century, and the Haber-Bosch production method and distribution network for ammonia are both well-established. A renewable energy source, such as solar energy, can also be used to create ammonia today [2]. In addition to its potential as a hydrogen energy vector, ammonia has a lot of appealing qualities as a fuel, including the ability to liquefy at low pressure (0.8 MPa) and ambient temperature [3]. This gives the transportation of NH_3 a significant safety and convenience advantage over other energy sources. As a result of its well-established production process and infrastructure, high hydrogen storage capacity, and accessible and affordable fuel characteristics, ammonia has enormous potential as a hydrogen energy vector. The current developments in the ecologically friendly and sustainable synthesis of NH_3 further increase its appeal as an energy source for the future. A cleaner and more effective energy environment could result from continued research and development in this field, opening up new avenues for innovation and economic expansion.

Since the 1960s, there has been a lot of research on NH_3 combustion, as shown in several scientific publications [4–9]. For instance, Verkamp et al.'s [4] experimental investigation on the quenching distance revealed that, under stoichiometric conditions, ammonia-air displayed a quenching distance that was 3.5 times larger than propane. Additionally, the laminar burning velocity of ammonia-air mixtures is quite modest, peaking at 6–8 cm/s at an equivalency ratio of around 1.1 [5–6]. Comparing this number to CH_4-air, it is approximately five times lower. It has been shown that the low laminar burning velocity prevents the utilization of both high inlet velocities and low inlet velocities to produce effective turbulent mixing and high combustion efficiency, respectively [7]. Additionally, because NH_3 contains a nitrogen atom, it may generate large amounts of nitrogen oxides (NO_X), which can be harmful [8–9]. Therefore, the main difficulty in NH_3 combustion is achieving a stable flame and low NO_X emissions.

According to numerous scholarly articles [10–14], researchers have investigated the use of hydrogen as an addition to improve the lower combustion intensity of ammonia. An experimental investigation was undertaken by Han et al. [10] to determine whether mixing NH_3 and H_2 would boost the laminar burning velocity of NH_3-containing fuel. The study found that the best strategy to increase the laminar burning velocity of NH3-containing fuel is to blend it with H_2. Additionally, it was discovered that fuel NO_X predominated, but thermal NO_X had a negligible impact on the burning of NH_3, H_2, and air [11]. Valera-Medina et al. [12-13] performed experiments for the NH_3/H_2 blend at the Gas Turbine Research Center. Their findings showed that in lean conditions, NO_X emissions are substantial due to the excessive formation of OH and O radicals, whereas under rich combustion conditions, comparatively low NO_X emissions are possible due to the presence of unburned NH_3. In a laboratory-scale swirl and bluff-body stabilized burner, Franco et al. [14] tested the combustion of NH_3/H_2/air while altering the equivalence ratio and NH_3 content. They proposed that NO_X is generated close to the burner input and then eliminated, perhaps through selective non-catalytic reduction. Overall, these investigations indicate that the addition of hydrogen may be a useful strategy for increasing ammonia's combustion intensity while also tackling the issue of NO_X emissions.

To employ ammonia-containing fuel in actual combustion equipment, it is essential to study the combustion characteristics of these fuels. Computational fluid dynamics (CFD) has been identified as an efficient method for analyzing the behavior of different critical species and radicals within the chamber. As reported in the literature [15–19], several research have been carried out to investigate the combustion of fuel containing NH_3 in different types of burners. In order to study the combustion of NH3 in a similar burner, Somarathne et al. [15] and Okafor et al. [16] used three-dimensional large eddy simulations. They discovered that the addition of secondary airflow can significantly minimize the amount of NO emissions. The combustion of NH_3-containing fuel in the Cardiff University swirl burner has been numerically explored by a number of research groups, including Honzawa et al. [18], who compared the NO content for the combustion of an NH_3/CH_4 blend under adiabatic and non-adiabatic conditions. The findings demonstrated a good agreement between predicted values and experimental values using a non-adiabatic flamelet-generated manifold method. The impact of heat loss was also examined by Vigueras-Zuniga et al. [19] using Reynolds Averaged Navier-Stokes (RANS) simulations. However, there is still a scarcity of studies that have focused on three-dimensional simulations of NH_3-containing fuel flames. Additionally, there has been little research examining the validity of turbulence combustion models, particularly the flamelet approach. Further studies are needed to develop a more comprehensive understanding of the combustion behavior of NH_3-containing fuels, which will facilitate the use of these fuels in practical combustion equipment.

In this study, large eddy simulation was employed using the dynamically thickened flame (DTF) model to validate the method by comparing the amount of NO produced. This study presents an investigation into the progression of the flame of a 50% NH_3/50% H_2 fuel mixture under lean premixed conditions in a swirl burner [20]. The flame structure was initially analyzed from the perspective of a one-dimensional simulation, followed by conducting large eddy simulations (LES) under two types of confinement conditions. The DTF model, an extension of the artificially thickened flame (ATF) model, which artificially thickens the flamelet, was used to characterize the flame structure using the LES grid.

The primary goals of this work are to offer new insights on combustion characteristics of NH_3-containing fuels and assess how well the DTF model predicts NO emissions. The accuracy of the simulations is confirmed by comparing the results with experimental data, which also helps to clarify the intricate physics underlying NH_3 combustion.

2. Numerical methods

2.1. Swirl burner and boundary condition

A large eddy simulation with finite rate chemistry was carried out using the OpenFOAM platform [21] in order to acquire a thorough three-dimensional understanding of the flame structure at lean conditions for a 50% NH_3/50% H_2 fuel blend. An overview of the burner and grid design used in the simulation is shown in Figure 1. The details regarding this burner can be found in previous studies [20, 22]. The fuel blend used in this investigation was 50% NH_3 and 50% H_2 by volume, with air serving as the oxidizer. This fuel blend was chosen due to its ability to produce a good laminar burning velocity similar to methane with near equivalent laminar burning velocity characteristics. Additionally, NO emissions were measured [22]. The NH_3/H_2/air mixture was supplied from the inlet with a constant equivalence ratio of 0.577. The wall condition was set to zero gradient for adiabatic

wall, while for non-adiabatic wall conditions, the wall temperature was fixed at the average of the inlet temperature and adiabatic flame temperature, which was 950K. Table 1 provides a summary of the boundary conditions used for the initial validation. The entire combustion chamber is computed using a structured mesh, which is generated using ICEM. Due to the study's focus on thermal boundary conditions, the quality of the mesh near the wall is crucial. The mesh is refined near the wall, with the grid size in this region being much smaller than the boundary layer thickness. This allows for a detailed resolution of the flow field structure near the wall when solving the boundary layer.

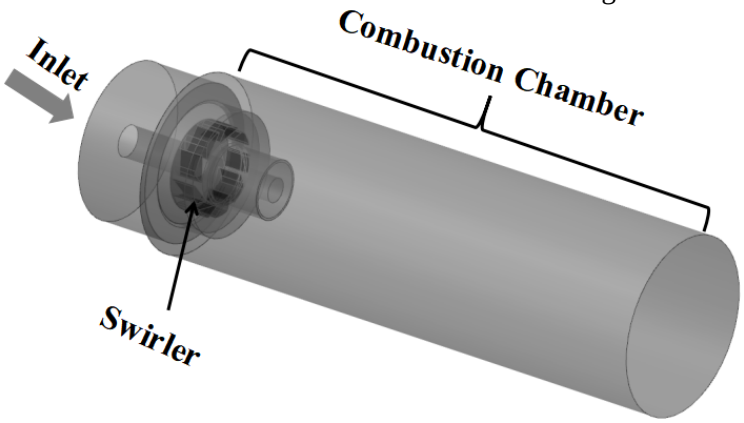

(a) Burner configuration

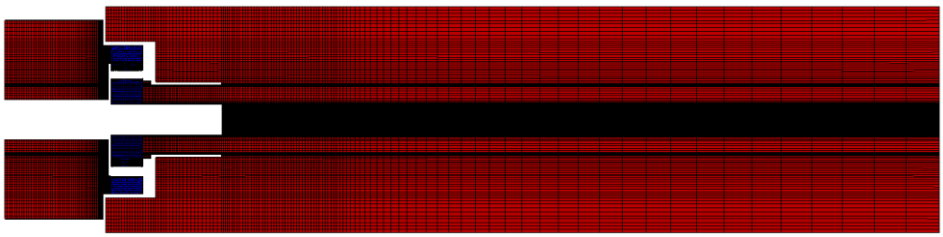

(b) Grid configuration

Fig. 1 Overview of burner configuration and grid configuration

Table 1. Boundary conditions

Operating Pressure	1atm	
Oxidiser (mol%)	O_2	21%
	N_2	79%
Fuel (mol%)	NH_3	50%
	H_2	50%
Mass Flow Rate (g/s)	NH_3	0.800
	H_2	0.094
	Air	14.001
Inlet Temperature	300K	
Wall Condition	Adiabatic, 950K	

2.2. DTF model and mechanism

The DTF model was proposed by Butler and O'Rourke [23]. This model modifies the exponential constants of the chemical reaction rate and thermal diffusion coefficient by a factor *F*. To

enable the resolution of the flame on an LES grid, the thickening factor $F_{dyn} = F(n_{dtf})$ is varied from large values inside the reaction zone to unity away from the flame front. An efficiency function E that may overcome the reduction of flame response to the smallest turbulent motions during the thickening process has been developed by Angelberger et al. [24] and Colin et al. [25]. This function *E* depends on the thickening factor F, the length scale $\Delta e/\delta_L^0$, and the velocity $u'_{\Delta e}/s_L^0$ ratios where Δe is the combustion LES filter size, δ_L^0 is the laminar flame thickness, $u'_{\Delta e}$ is the subgrid scale rms velocity, and s_L^0 is the laminar burning velocity.

Three global variable parameters need to be predetermined when utilizing the DTF model to handle the interaction between turbulence and chemistry: 1) global grid thickening coefficient n_{dtf}, 2) laminar flame thickness δ_L^0, and 3) laminar burning velocity s_L^0. After 1D premixed free propagated flame simulation, The δ_L^0 and s_L^0 are 1 mm and 0.126 m/s, respectively, following a simulation of a 1D premixed free propagating flame. Wang et al. [26] employed the DTF model to study the CH_4/air flame with an equivalence ratio of 0.75 and 0.83 at the atmosphere. The analysis demonstrates that numerical results using the small thickening coefficient (n_{dtf}=2.5~5) in the dynamic thickening process are in good agreement with the experimental findings. Premixed CH4/air laminar flame has a flame thickness in the range of 1- 2 mm, which is comparable to the 50% NH_3/50% H_2 fuel blend's laminar flame thickness at f = 0.577 calculated above. Hence, this paper uses the thickening coefficient proposed by Wang et al. [26] and adopts the thickening coefficient n_{dtf}=5.

The non-linear chemical kinetics equations must be coupled to fluid dynamics and transport phenomena in order to simulate the combustion process. As this can be a time-consuming process, it is often necessary to use reduced mechanisms to minimize computational time. The NH_3/H_2 mechanism developed by Xiao et al. [27] is a good example of such a reduced mechanism. Excellent agreement in the laminar burning velocity is shown by this approach, which also requires a lot less computing time [28]. Therefore, the NH3/H2 mechanism, which consists of 24 species and 91 steps, was applied in this study to model the chemical kinetics.

2.3. 1D numerical studies

One-dimensional premixed free propagating flame calculations were carried out with Cantera [29] to better understand the flame structure. CHEMKIN-PRO [30] was used to determine the impact of recirculation strength and heat loss on the final NO emission. A chemical reactor network (CRN) approach was used to model the swirling flame with a recirculation zone, as shown in Figure 2. The CRN used in this study consists of a hybrid perfectly stirred reactor (PSR), a plug flow reactor (PFR), and a partially stirred reactor (PaSR), which are composed of four sections. Two inlets were utilized to provide a 50% NH_3/50% H_2 fuel mixture and an air/water vapor mixture, while three PSRs were employed to simulate the premixed zone, premixed flame, and central recirculation zone. The post-flame region was modeled using a one-dimensional PFR with a length of 5 cm. The PaSR was designed to simulate the extinguishment/mixing zone of the main combustion products and secondary air flow. The lean zone was simulated using the second PFR, which had an axial length of 5 cm. An NH_3/H_2 fuel mixture's main combustion zone typically has a residence duration of a few milliseconds, and the generation of NO_X there is not very sensitive to the residence time. As a result, the primary flame zone's residence time in this investigation was set at 1.5 ms. The two PFRs employed in this investigation have sufficient one-dimensional length since the NO_X concentration rapidly drops in the

front of the PFR and stabilizes in the back. The researchers were able to develop a thorough grasp of the combustion process and flame structure by utilizing these different methods.

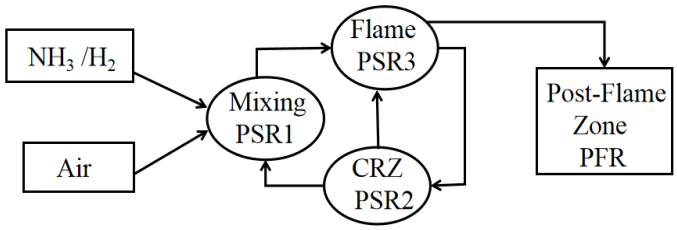

Fig. 2 PSR-PFR schematic

3. Results and discussion

3.1. One-dimensional flame simulation using cantera

The one-dimensional structure of a laminar premixed flame at an equivalence ratio of 0.577 is depicted in Figure 3. The flame thickness is approximately 1 mm, and the flame temperature is about 1620K. Since the flame temperature is below 1800K, which is the critical temperature to generate thermal NO, fuel NO predominates in the ultimate NO emission. When the curves between NH3 and H2 are compared, it can be seen that H2 reacts more quickly and produces a bigger reaction zone than NH3 due to the higher hydrogen diffusion and consumption rates. Additionally, as shown in Figure 3(a), the mole fraction of H_2 is somewhat higher than that of NH3 during burning, most likely as a result of NH_3 breaking down into H_2. The NO mole fraction is approximately 0.0062 from the 1D laminar numerical calculation. The formation of NO is sensitive to the content of OH, O, and H radicals [31], which is consistent with the trend of OH, O, and H radicals and NO, as shown in Figure 3(b). The OH, O, and H radicals reach a peak near the flame front, and NO is also generated around the flame front. Moreover, the decomposition of NH_3 is related to the content of OH, O, and H radicals [32], with OH radicals playing the most important role. H_2 can improve the combustion properties of pure NH3, most likely as a result of the reaction between H_2 and O_2 that produces the OH, O, and H radicals.

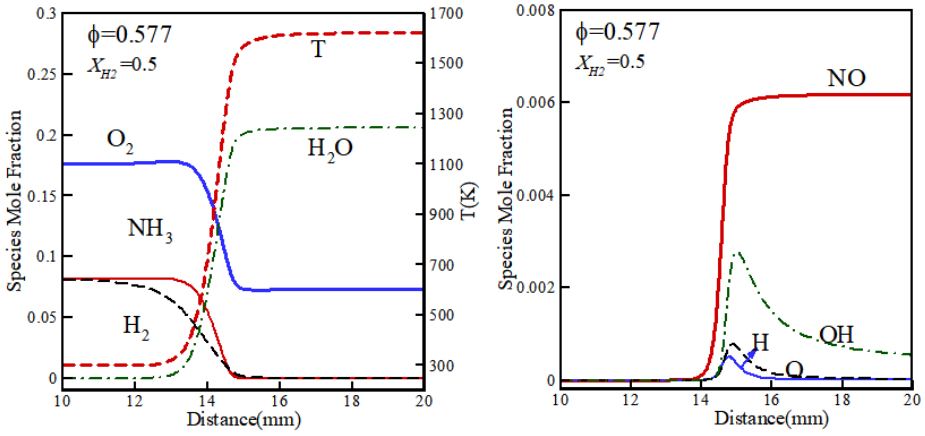

(a) **(b)**

Fig. 3 Predicted structure of a premixed laminar free propagated NH_3/H_2 flame at equivalent ratio of 0.577

NO emissions are a major concern when using ammonia-containing fuel in practical combustion devices. Figure 4 illustrates the impact of recirculation zone ratio and heat loss ratio on NO emissions. Figures 4(a) and 4(b) vary the recirculation zone ratio under adiabatic conditions, while Figures 4(c) and 4(d) vary the heat loss ratio at a recirculation zone ratio of 0.2. Increasing the recirculation zone ratio and heat loss ratio can reduce the absolute NO production rate, resulting in a decrease in NO emissions. Figure 4(b) illustrates how the effect of the recirculation zone ratio on the flame temperature and OH concentration can be disregarded. Thus, the increase in NO production rate and emissions is caused by the entrance of more flue gas into the recirculation zone, leading to an increase in NO in the flame zone. On the other hand, increased heat loss decreases the concentration of OH radicals, which are reactants for NO formation, resulting in a reduction of NO emissions. Furthermore, as Figures 4(b) and 4(d) indicate, the flame temperature and OH mole fraction exhibit a positive correlation relationship.

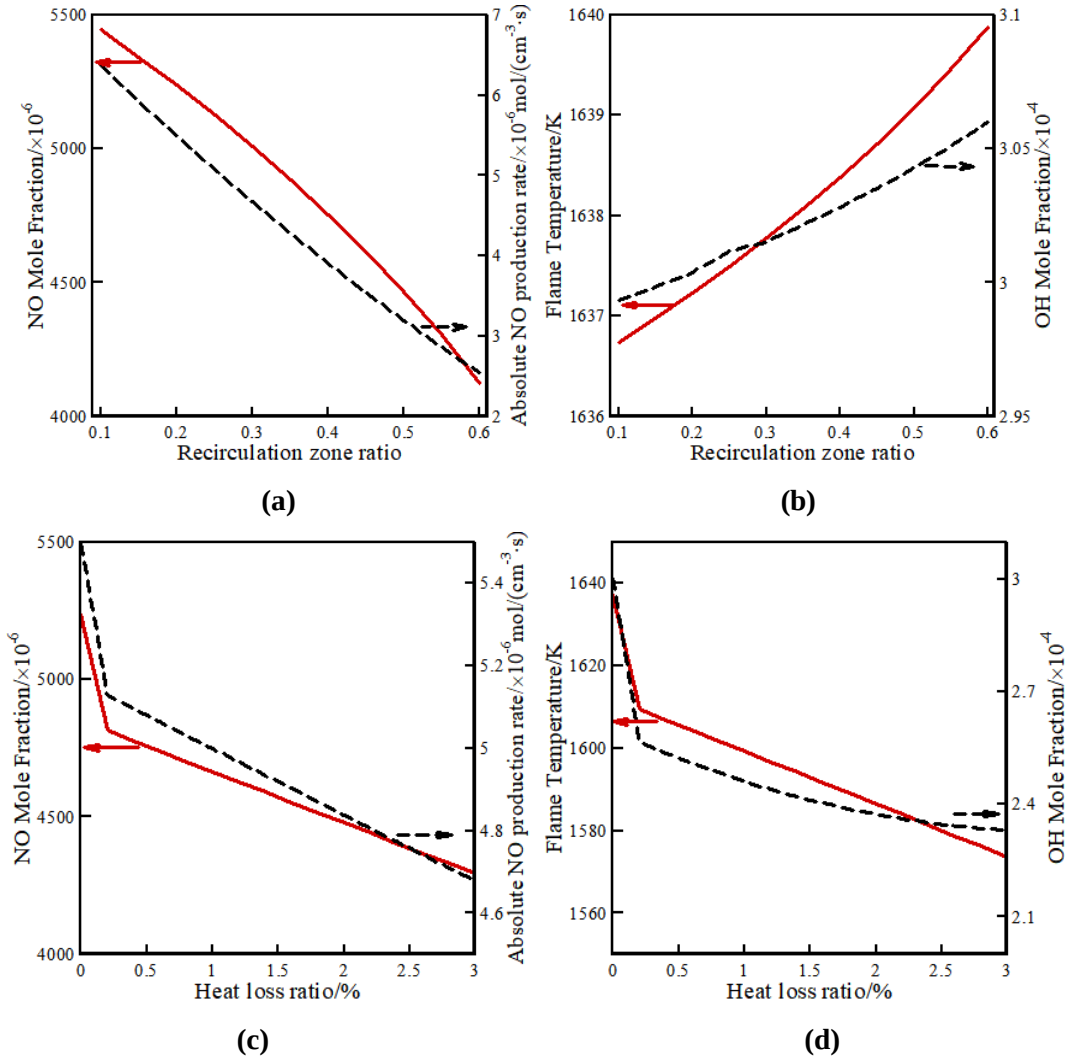

Fig. 4 Effect of recirculation zone ratio and heat loss ratio on NO emission, flame temperature and OH mole fraction

3.2. Analysis of velocity field under large eddy simulation

Two hybrid computational meshes with 1.4 million (coarse) and 2.67 million (fine) cells each were generated to conduct a grid independence study. The unstructured cells were used in the swirl section, while structured cells were used in other parts of the mesh. Additionally, small cells were also provided to alleviate the turbulent eddies in the recirculation zone around the axial area. The axial distribution diagram of burner temperature and NO mole fraction was simulated to ascertain the grid's appropriateness, as shown in Figure 5. There was a recurring pattern when the two grid sets were compared. In contrast to the coarse grid, the fine grid had a more erratic flame position. This phenomenon can be attributed to the fine grid's sensitivity to temperature and NO emissions. Considering the trade-off between calculation accuracy and speed, the fine grid was ultimately selected for this study.

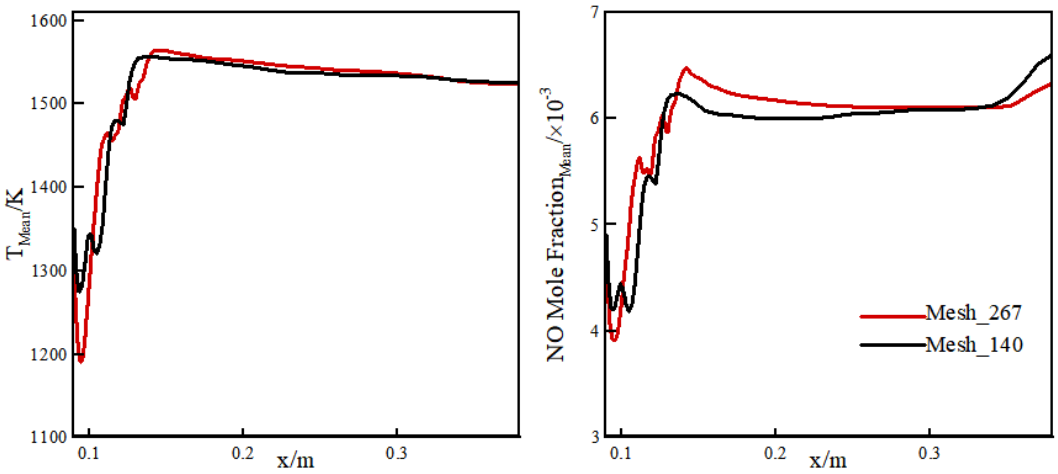

Fig. 5 Comparison of calculated values for two sets of grids; (a) Averaged temperature, (b) Averaged NO mole fraction

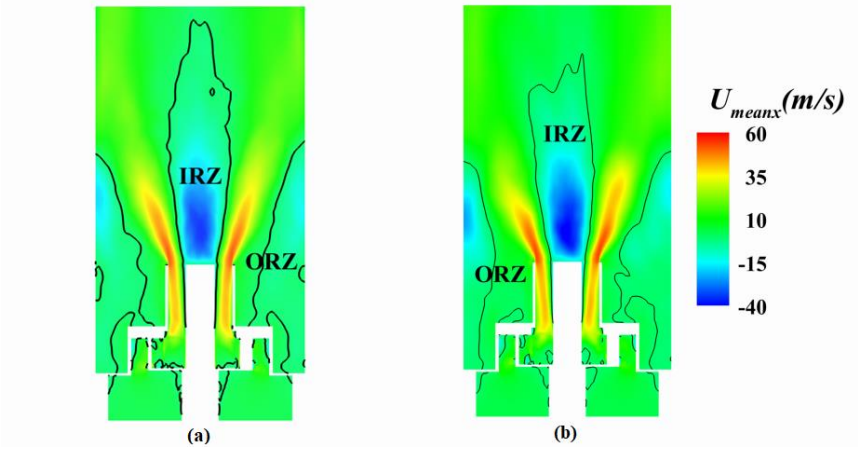

Fig. 6 Comparison of axial average velocity at adiabatic and non-adiabatic wall conditions (a) Non-adiabatic axial average velocity, (b) Adiabatic axial average velocity

In this study, an approach using 2D cloud image slices and section position analysis was utilized to investigate the effect of heat loss on the combustion characteristics of ammonia/hydrogen premixed

flames. It is essential to clarify that the solid line represents the axial average velocity where the speed is zero. The recirculation zone includes various components such as the internal recirculation area (IRZ) and the external recirculation area that is surrounded by the zero-gradient line. As shown in Figure 6, a significant phenomenon is observed where the free radicals and hot combustion gas are brought by recirculation into the upstream region of the combustion chamber. This leads to the mixing of combustion and unburned gases in the return zone, thereby maintaining a continuous chemical reaction under the influence of a strong swirling flow. The recirculation zone acts as a carrier of heat and mass, which plays a vital role in the overall combustion process. The detailed analysis of the recirculation zone and its impact on the combustion process is critical for the optimal design and operation of practical combustors.

Figure 7 displays the average temperature under two wall conditions to examine the impact of heat loss. The axial velocity averages of various sections along the radial direction are compared under two conditions: adiabatic condition (zero-gradient) and wall temperature of 950K. The five axial distances correspond to the height from the flame root to the top (x=0.09, 0.11, 0.13, 0.15, 0.17, 0.19m). Several similarities between the two wall conditions can be observed. The average velocity at the flame center is nearly identical, but the velocity near the wall differs. As shown in Figure 6, the strength of the internal recirculation zone is significantly greater than that of the external recirculation zone, indicating that the total recirculation strength is determined by the internal recirculation strength. As the flame develops downstream, the internal recirculation increases, reaching the maximum value at the axial position of 0.11m (in the middle of the flame) as the recirculation speed decreases. Furthermore, the closer to the flame root, the greater the axial velocity gradient of the outer layer of the internal circulation zone, indicating that the shear layer mixing of fresh mixture and gas in the internal circulation zone is more intense.

Figure 7 shows that at the flame root (Δ=90mm), the reflux velocity is slightly increased under the diabatic condition. At Δ=110mm and Δ=130mm, there is almost no difference, which is caused by the influence of the central part of the flame. At the flame head (Δ=150mm, Δ=170mm, and Δ=190mm), the flame temperature further increases, and the external recirculation zone almost disappears. In summary, these results show that the main factor affecting the recirculation intensity is the flame part, and the external recirculation zone is less influenced by the wall temperature conditions than the internal recirculation zone.

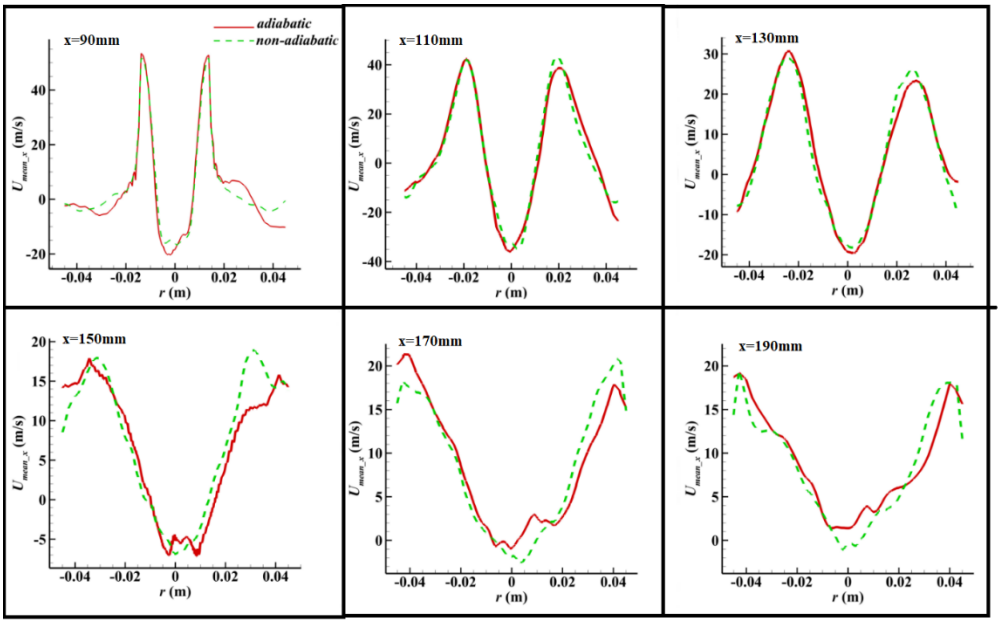

Fig. 7 Comparison of the radial average velocity at different axial locations for non-adiabatic and adiabatic conditions, Δx=90mm,110mm,130mm,150mm,170mm,190mm

3.3. Analysis of temperature field and component field in large eddy simulation

The results of our study reveal that NH_3 propagates downward along the axial velocity and becomes enriched at the peak axial velocity position, as demonstrated in Figure 9 (a). On the other hand, OH is predominantly formed in the internal recirculation zone, as illustrated in Figure 9 (c), and subsequently mixed with the fresh mixture via the internal shear layer to oxidize NH_3 and H_2. The valley region of NO mole fraction is located exactly in the peak region of axial velocity (Figure 10 (d)) owing to the presence of unburned gas in this region.

Given that NO formation is sensitive to OH free radicals, the distribution of OH concentration in the internal recirculation zone corresponds with that of NO. Through the evaluation of temperature and OH mole fraction, the vortex flame structure of 50% NH_3 /50% H_2 under lean condition f=0.577 has been discussed, as displayed in Figure 8 and Figure 9 (c). Our analysis shows that the flame height is approximately 40mm, which agrees with previous experimental results when f=0.43 (~45mm) and f=0.52 (~42mm) [12].

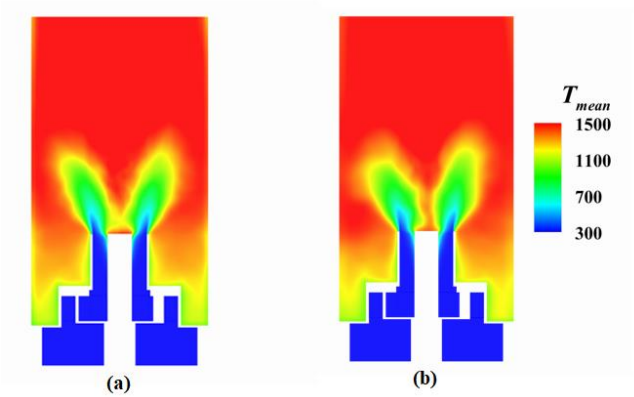

Fig. 8 Comparison of axial average temperature at adiabatic and non-adiabatic wall conditions (a) Non-adiabatic axial average temperature, (b) Adiabatic axial average temperature

The temperature distribution within the flame zone is a critical factor in understanding the behavior of combustion processes. As discussed in Figure 9 and Figure10, under adiabatic conditions, the temperature is uniformly distributed within the flame zone, hovering around 1600K. However, non-adiabatic conditions result in a non-uniform temperature distribution, causing a 50K reduction in temperature compared to adiabatic conditions. The flame topology is characterized by the position with high OH concentration, indicating that an “M” flame topology is generated by eddy currents and bluff bodies.

Figure 9 (c) and Figure 10 illustrates that OH radicals collect at the flame front, suggesting that they are formed and consumed at the flame front. The outer edge of the OH profile corresponds to the velocity distribution and is irregular. Under adiabatic conditions, OH radicals exist throughout the entire combustion chamber downstream of the flame, while under non-adiabatic conditions, the OH content shows a gradient from the wall to the combustion chamber due to heat loss. As a result, the temperature near the wall is lower than the temperature required for OH formation. NH_3 propagates downward along the axial velocity and becomes enriched at the peak axial velocity position, while OH is primarily formed in the internal recirculation zone, mixed with the fresh mixture, and used to oxidize NH_3 and H_2. The valley region of NO mole fraction corresponds to the peak region of axial velocity due to the presence of unburned gas. The distribution of OH concentration in the internal recirculation zone is consistent with that of NO, which is formed due to OH free radicals.

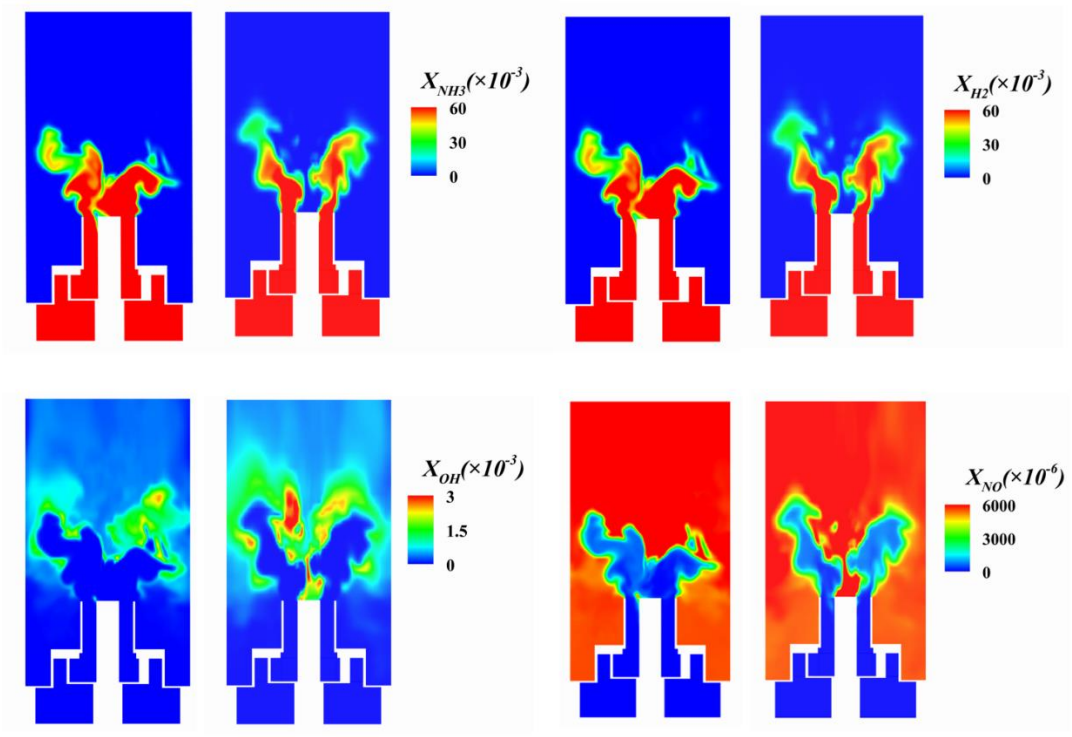

Fig. 9 Comparison of transient components NH_3/H_2/OH/NO under non-adiabatic and adiabatic wall conditions

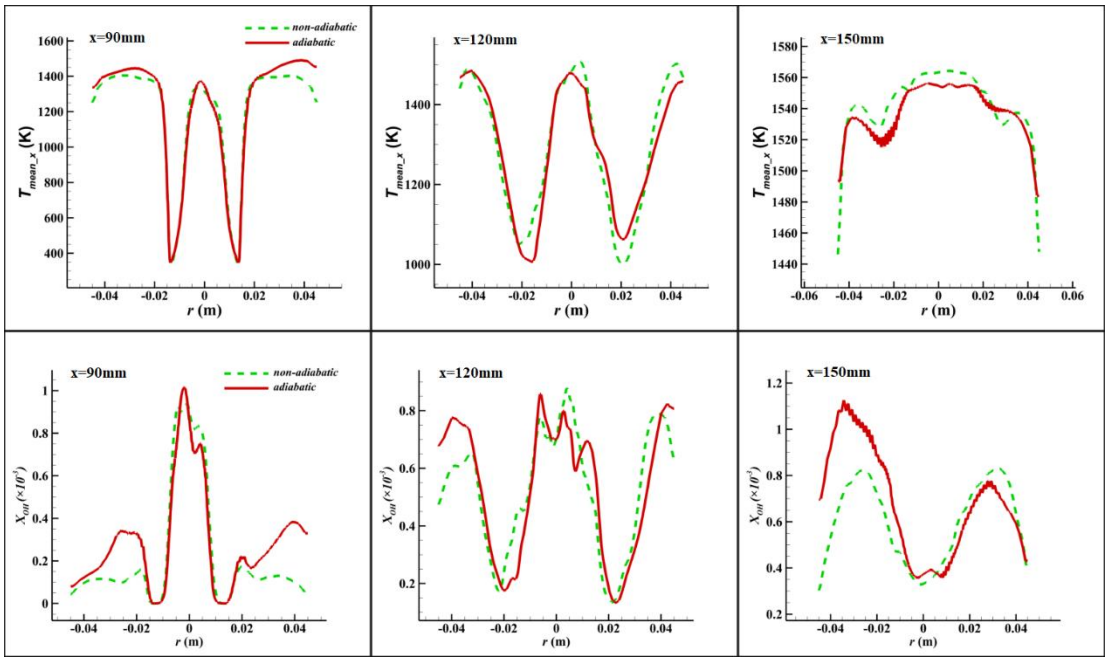

Fig.10 Comparison of the radial average temperature and OH components at different axial locations for non-adiabatic and adiabatic conditions, Δx=90mm,120mm,150mm

In Figure 9, the mole fractions of NH_3, H_2, OH and NO are represented, respectively. The reaction regions of NH3 and H_2 are marked without blue, with the reaction region of H_2 being slightly larger than that of NH_3, consistent with the structure of a one-dimensional premixed free diffusion flame. Additionally, the concentration of NO in the external recirculation zone is lower than that in the flame zone, primarily due to the dilution of NO concentration by cold air in the external recirculation area. NO is predominantly produced at the front of the flame, where NH_3 is oxidized to HNO radicals, and OH radicals are enriched. Fuel NO is formed through the consumption of HNO and OH radicals. Finally, the distribution of NO under non-adiabatic conditions shows that NO is formed at the front of the flame, with the NO mole fraction and flame zone temperature under non-adiabatic conditions being lower than those under adiabatic conditions, indicating that fuel NO is sensitive to temperature.

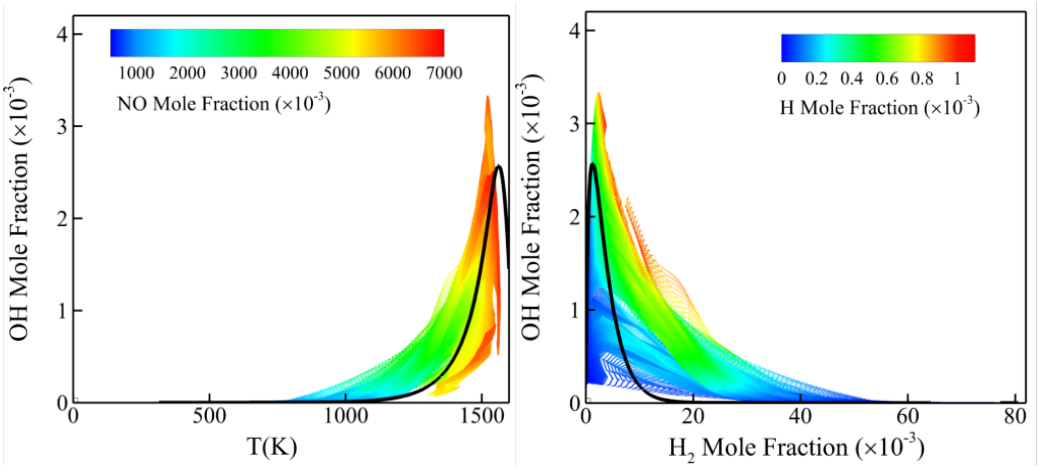

(a) (b)

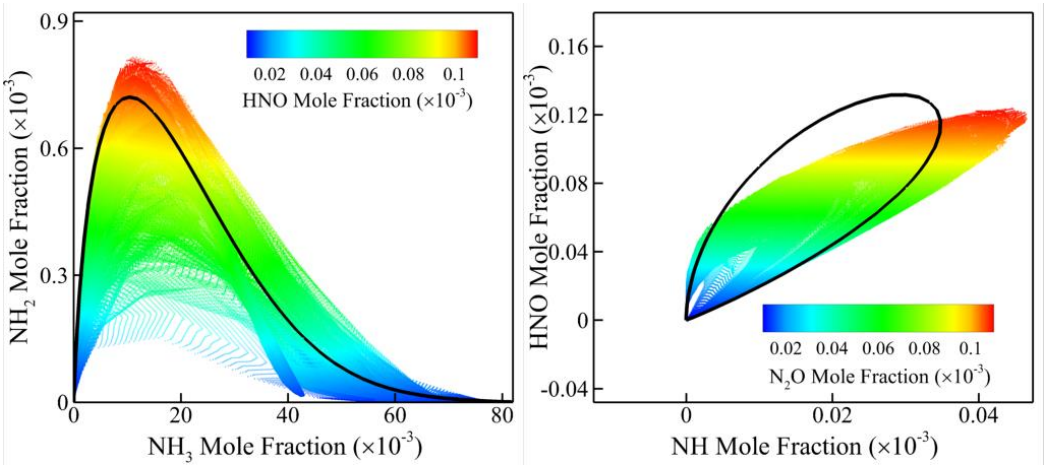

(c) (d)

Fig. 11 Scatter plots: (a) T- OH mole fraction, (b) H_2 mole fraction- OH mole fraction, (c) NH3 mole fraction- NH_2 mole fraction, (d) NH mole fraction- HNO mole fraction

Figure 11 shows the instantaneous distribution of the mole fractions of NH_3, H_2 and NO of the main species. Under inlet conditions, the molar ratio of ammonia and hydrogen is 1:1, resulting in almost the same distribution of ammonia and hydrogen. In Figure 11, the scatter plots illustrate the relationships between the concentrations of various species and temperature at the flame front zone. It becomes apparent that at flame temperatures below 1600K, thermal NO can be disregarded, and Fuel NO is formed in the zone of high temperature and OH concentration, as demonstrated in Figure 11 (a). The formation of OH radicals is highly temperature-sensitive, and thus flame temperature plays a pivotal role in determining fuel NO content. Moreover, a small amount of H_2 is involved in the formation of H and OH radicals, as depicted in Figure 11 (b), which exhibits a positive correlation between H and OH concentrations.

In addition, the maximum concentrations of NH2 and HNO are achieved when the NH3 mole fraction is approximately 20×10^{-3}. Figure 11 (c) displays a positive correlation between NH2 and HNO concentrations, which can be explained by the NH3 decomposition path NH3→ NH_i(i=0,1,2) → HNO. N_2O is clearly correlated with NH_2 and HNO, as illustrated in Figure 11 (d). N2O is the reduction product of NO, and HNO radical is a crucial intermediate species for the formation of NO. NH_2, as an oxide, participates in the reduction of NO to form N_2O. When the HNO concentration is high and the NH_2 concentration is low, a large amount of NO will be generated, but NO cannot be reduced to N_2O due to the lack of NH_2. On the other hand, when the concentration of HNO and NH_2 is at a fixed proportion, these two radicals precisely promote the formation of N_2O.

3.4. Analysis of reflux intensity and comparison of large eddy simulation and CRN simulation and experimental results

In this paper, reflux intensity is defined as the proportion of reflux mass flow to total mass flow. The increase of reflux intensity can reduce NO emission. Therefore, the reflux intensity is an important parameter for the design of burner burning NH_3 fuel. The reflux intensity used by Cardiff University in the CRN numerical calculation is usually obtained by fitting the experimental value with the simulated value. In this paper, detailed flow field information can be obtained in large eddy simulation, so relatively accurate reflux intensity can be obtained for future burner design and CRN numerical simulation.

According to the actual combustion situation, referring to the velocity field under large eddy simulation under non-adiabatic conditions, the reflux intensity will reach a maximum of 65% in the flame development section. According to the above analysis, the reflux intensity will affect the re-reaction of the inhaled flue gas, and the NO in the flue gas will also be brought back to the reaction zone, which will increase the NO concentration in the reaction zone, so as to reduce the NO emission.

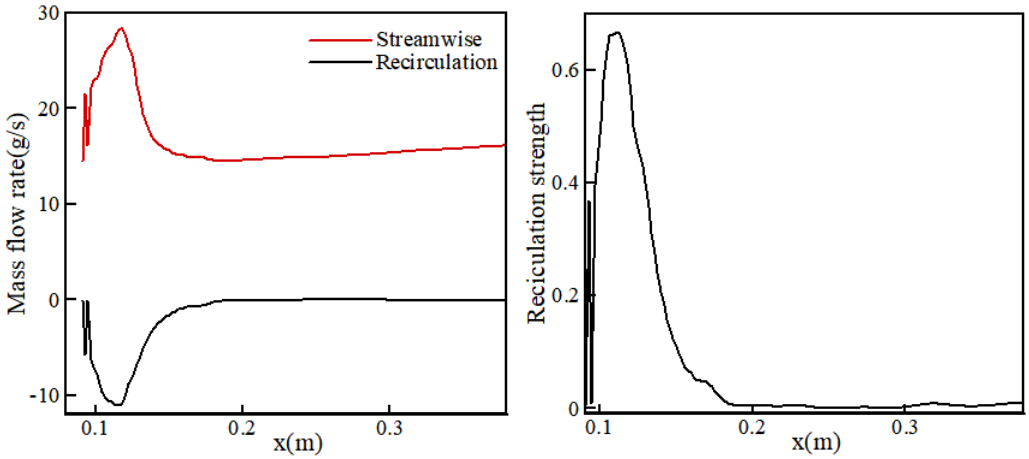

Fig. 12 Mass flow rate and recirculation strength along the axis line for non-adiabatic condition, (a) mass flow rate, (b) recirculation strength

Based on the analysis presented above, the heat loss rate and reflux strength have been considered as important parameters in the context of CRN. In order to compare the numerical results obtained from CRN, LES, and experimental data, these two parameters have been applied in the CRN, and the results have been illustrated in Fig. 13. It is worth noting that the NO concentrations predicted by LES are higher than those obtained in the experiment, whereas the CRN tends to underestimate the NO emission. It has been observed that the LES, which takes into account the non-adiabatic conditions, can predict the NO emission more accurately. On the other hand, the CRN, which considers the heat loss ratio and recirculation strength calculated by LES, shows a good agreement with the experimental results.

The reason for this difference in the results can be attributed to the fact that the CRN analysis is only focused on the chemical reaction, which represents the ideal state of gas combustion. In contrast, the actual experiment involves other physical parameters and the error associated with the experiment itself. Furthermore, it has been observed that under large eddy simulation, the gas reaction on the adiabatic wall is more complete and the combustion temperature is higher, which leads to a greater NO emission than under non-adiabatic wall conditions. This can be attributed to the influence of the temperature field on gas reaction. Based on these findings, it can be concluded that reducing the reaction temperature can effectively reduce the NO emission.

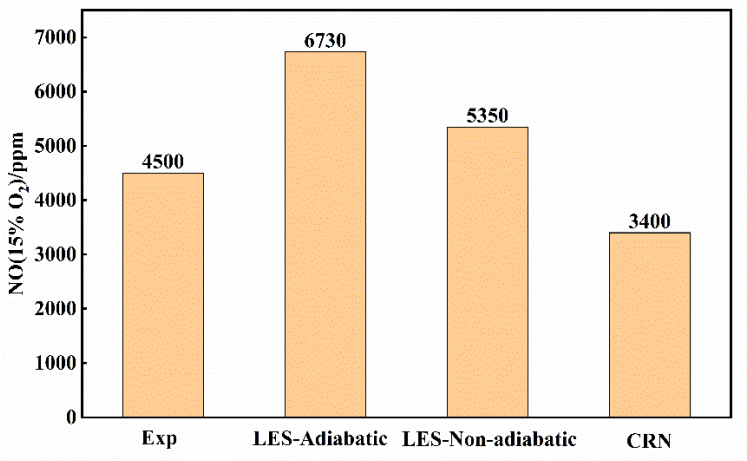

Fig. 13 Comparison of amounts of NO emission (15% O_2) at f=0.577 among LES results of adiabatic, non-adiabatic and CRN result, together with experiments

4. Conclusions

In the present investigation, a LES approach was employed utilizing the DTF model to examine the combustion characteristics of NH_3/H_2/air fields generated by a swirl burner. This study provides a detailed investigation of the underlying mechanisms of these combustion fields. The key findings of the study are summarized as follows.

1. At lean condition f = 0.577, the flame height and flame thickness of 50% NH_3/50% H_2 were 40mm and 0.8mm, respectively.

2. The recirculation zone was located at the flame position, and the inner recirculation strength played a decisive role in determining the total recirculation strength. The maximum recirculation strength of 0.65 was observed at the middle of the flame.

3. H_2 reacts first and generates a larger reaction zone than NH_3. Additionally, H and OH radicals are positively correlated, while there is some positive correlation between NH_2 and HNO. Furthermore, as the reduction product of NO, the concentration of N_2O is controlled by the concentration of HNO and NH_2 radicals.

4. OH radicals are predominantly formed in the inner recirculation zone, while NO is produced at the flame front. Furthermore, NO emission is through the fuel NO path, which is highly sensitive to flame temperature.

5. Reducing the combustion temperature can effectively reduce NO emission.

In summary, this study sheds light on the intricate details of NH_3/H_2/air combustion fields and provides valuable insights that can inform the development of more efficient and environmentally friendly combustion technologies.

Acknowledgment

The authors gratefully acknowledge the generous support provided by the Natural Science Foundation of China (NSFC) under Grant No. 91741117, and the High-tech Research Key Laboratory of Zhenjiang (No. SS2018002). The Support by the State Key Laboratory of Clean Energy Utilization (Open Fund Project No. ZJUCEU2022020) is also acknowledged. The authors also thank Prof. Agustin Valera-Medina and his team (Cardiff University, UK) for providing the experimental results.

References

[1] Chiuta, S, *et al*., Reactor technology options for distributed hydrogen generation via ammonia decomposition: a review, *Int J Hydrogen Energy, 38* (2013), pp. 14968-14991

[2] Michalsky, R., *et al.*, Solar thermochemical production of ammonia from water, air and sunlight: thermodynamic and economic analyses, *Energy, 42* (2010), pp. 251–260

[3] Yang, S. J., *et al*., Recent advances in hydrogen storage technologies based on nanoporous carbon materials, *Prog Nat Sci, 22* (2012), pp. 631-638

[4] Verkamp, F. J., *et al*., Ammonia combustion properties and performance in gas turbine burners. *Int Symp Combust, 11* (1967), 1, pp. 985-992

[5] Lee, J. H., *et al*., Effects of ammonia substitution on hydrogen/air flame propagation and emissions, *Int J Hydrogen Energy, 35* (2010), pp. 11332–11341

[6] Kumar, P., *et al*., Experimental and modeling study of chemical-kinetics of mechanisms for H_2–NH_3–air mixtures in laminar premixed jet flames, *Fuel, 108* (2013), pp. 166–176

[7] Pratt, D. T., Performance of ammonia fired gas turbine combustors, Report TR-9-TS-67-5. Solar San Diego, California: USA; 1967

[8] Mathieu, O., *et al*., Experimental and modeling study on the hightemperature oxidation of ammonia and related NO_X chemistry, *Combust Flame, 162* (2015), pp. 554-570

[9] Hayakawa, A., *et al*., Experimental investigation of stabilization and emission characteristics of ammonia/air premixed flames in a swirl combustor, *Int J Hydrogen Energy, 42* (2017), 19, pp. 14010-14018

[10] Han, X. L., *et al*., Experimental and kinetic modeling study of laminar burning velocities of NH3/air, NH3/H2/air, NH3/CO/air and NH3/CH4/air premixed flames, *Combust Flame, 206* (2019), pp. 214-226

[11] Li, J., *et al*., Study on using hydrogen and ammonia as fuels: combustion characteristics and NO_X formation, *Int J Energy Research, 38* (2014), 9, pp. 1214-1223

[12] Valera-Medina, A., *et al*., Preliminary study on lean premixed combustion of ammonia-hydrogen for swirling gas turbine combustors, *Int J Hydrogen Energy, 42* (2017), pp. 24495-24503

[13] Valera-Medina, A., *et al*., Premixed ammonia/hydrogen swirl combustion under rich fuel conditions for gas turbines operation, *Int J Hydrogen Energy, 44* (2019), pp. 8615-8626

[14] Franco, M. C., *et al*., Characteristics of NH_3/H_2/air flames in a combustor fired by a swirl and bluff-body stabilized burner, *Proc Combust Inst, 38* (2021), 4, pp. 5129-5138

[15] Somarathne, K. D. K. A., *et al*., Numerical study of a low emission gas turbine like combustor for turbulent ammonia/air premixed swirl flames with a secondary air injection at high pressure, *Int J Hydrogen Energy, 42* (2017), 44, pp. 27388-27399

[16] Okafor, E. C., *et al*., Towards the development of an efficient low-NO_x ammonia combustor for a micro gas turbine, *Proc Combust Inst,* 37 (2018), 9, pp. 4597-4606

[17] Xiao, H., *et al*., 3D simulation of ammonia combustion in a lean premixed swirl burner, *Energy Procedia, 142* (2017), pp. 1294-1299

[18] Honzawa, T., *et al.*, Predictions of NO and CO emissions in ammonia/methane/air combustion by LES using a non-adiabatic flamelet generated manifold, *Energy, 186* (2019), 115771

[19] Vigueras-Zuniga, M. O,. *et al.*, Numerical predictions of a swirl combustor using complex chemistry fueled with ammonia/hydrogen blends, *Energies, 13* (2020), 2, 288

[20] Valera-Medina, A., *et al.*, Ammonia, Methane and hydrogen for gas turbines, *Energy Procedia, 75* (2015), pp. 118-123

[21] OpenFOAM 1.7.1. 2010. Available at: http://openfoam.org/version/1-7-1/.

[22] Runyon, J., *et al.*, Methane-oxygen flame stability in a generic premixed gas turbine swirl combustor at varying thermal power and pressure, *ASME turbo expo,* 2015GT2015-43588

[23] Butler, T. D., *et al.*, A numerical method for two-dimensional unsteady reacting flows, *Proc Combust Inst, 16* (1977), pp. 1503-1515

[24] Angelberger, C., *et al*., Large eddy simulation of combustion instabilities in turbulent premixed flames, *Proceedings of the Summer Program,* (1998), pp. 61-82

[25] Colin, O., *et al*., A thickened flame model for large eddy simulations of turbulent premixed combustion, *Physics of Fluids, 12* (2000), 7, pp. 1843-1863

[26] Wang, P., *et al*., A detailed comparison of two sub-grid scale combustion models via large eddy simulation of the PRECCINSTA gas turbine model combustor, *Combust Flame, 164* (2016), pp. 329-345

[27] Xiao, H., *et al*., Modeling combustion of ammonia/hydrogen fuel blends under gas turbine conditions, *Energy Fuels, 31* (2017), 8, pp. 8631-8642

[28] Mao, C. L., *et al*., Laminar flame speed and NO emission characteristics of premixed flames with different ammonia-containing fuels, *J Chem Ind Eng (China), 72* (2021), 10, pp. 5530-5543

[29] Goodwin, D. G., Moffat, H. K., Speth, R. L., Cantera. http://www.cantera.org

[30] ANSYS CHEMKIN PRO version 18.1. http://www.ansys.com/products/fluids/ansys-chemkin-proANSYS

[31] Rocha, R. C. D., *et al*., Chemical kinetic modelling of ammonia/hydrogen/air ignition, premixed flame propagation and NO emission, *Fuel, 246* (2019), pp. 24-33

[32] Kumar, P., Meyer, T. R., Experimental and modeling study of chemical-kinetics mechanisms for H_2-NH_3-air mixtures in laminar premixed jet flames, *Fuel, 108* (2013), pp. 166-176

Received: 23.11.2023.

Revised: 27.06.2024.

Accepted: 18.12.2024.